Int J Clin Exp Pathol 2017;10(9):9132-9145
www.ijcep.com /ISSN:1936-2625/IJCEP0057690

Original Article

Role of β_3 adrenoceptor in rat thoracic aorta contractility

Qianqian Zhao[1*], Huanzhen Chen[2*], Jiani Jing[1], Xi Wang[1], Rong Liu[1], Xiaopeng Li[1], Haiqing Li[1], Xiangli Cui[1]

[1]Department of Physiology, Shanxi Medical University, Taiyuan, Shanxi, China; [2]Department of Cardiology, First Hospital of Shanxi Medical University, Taiyuan, Shanxi, China. [*]Equal contributors.

Received May 18, 2017; Accepted July 13, 2017; Epub September 1, 2017; Published September 15, 2017

Abstract: To clarify the role of β_3-AR in rat thoracic aorta contractility and underlying mechanisms. BRL 37344 (BRL) was used to detect the role of β_3-AR on rat thoracic aorta. 40 rats were randomly divided into Sham control group, Sham+SR group with SR 59230A (SR) injected, chronic heart failure (CHF) control group, and CHF+SR group. The effects of SR on thoracic aorta structure, function and NF-κB expression were estimated. BRL produced relaxant effect in both endothelium-intact and endothelium-free aorta rings, which was antagonized by SR and partially by L-NAME, but not changed by Propranolol. Similar results were obtained on thoracic aorta smooth muscle of CHF rats. β_3-AR was located in both vascular smooth muscle layer and endothelial layer. After SR injection, the aorta rings in Sham+SR group showed reduced endothelium-dependent relaxation response to Ach compared with Sham control group. The aorta rings in CHF control group showed reduced endothelium-dependent relaxation to Ach, with increased endothelium-dependent relaxation in CHF+SR group. Besides, SR injection showed increased contraction to NA. Meanwhile, NF-κB expression in Sham+SR group was higher than Sham control group, with increased expression in CHF control group but decreased in CHF+SR group. Microarray screening showed 48 and 42 differentially expressed miRNAs in Sham+SR rats and CHF+SR rats respectively with 19 of them associated with NF-κB pathways. β_3-AR is expressed in rat aorta and exerts relaxant effects through NOS-dependent pathway. β_3-AR Inhibition delayed damage of vessels in development of heart failure possibly through regulation of NF-κB signaling pathway.

Keywords: Rat, thoracic aorta, β_3 receptor, BRL 37344, SR 59230A, heart failure, endothelial function

Introduction

Besides β_1 and β_2 adrenoceptors, the function of a new β adrenoceptor subtype, β_3 adrenoceptor (β_3-AR) in cardiovascular system had drawn attention to researchers. β_3-AR was cloned in 1989 and firstly found in adipose tissues where it plays an important role in the regulation of lipid metabolism [1, 2]. Later on, β_3-AR was also found in gastrointestinal and airway smooth muscle [3, 4]. β_3-AR was discovered in human heart in 1996 and plays the negative inotropic effect [5, 6], β_3-AR was also found in urinary smooth muscle and reproductive system and induced a relaxant effect [7, 8].

A previous study demonstrated that concentration-dependent vasorelaxation in rat thoracic aorta caused by SR 58611 (a preferential β_3-AR agonist) was not modified by pre-treatment with nadolol (a β_1/β_2-AR antagonist) but antagonized by SR 59230A, a β_3-AR antagonist [9]. However, the role of β_3-AR in mediating relaxation in rat aorta had been challenged by MacDonald A group whose studies showing evidence against beta 3-adrenoceptors or low affinity state of beta 1-adrenoceptors mediating relaxation in rat isolated aorta [10, 11]. To settle this dispute, in this study, we explored the inotropic effect of β_3-AR on thoracic aorta by localizing the β_3-AR expression, exploring the function and the related signaling pathway of β_3-AR in rat aorta.

Chronic heart failure (CHF) is the terminal stage of various cardiovascular diseases. Though myocardial cell apoptosis, inflammatory response and ventricular remodeling were involved in the development of heart failure, excessive activation of the sympathetic adrenal system which target adrenaline receptors is one of

the important changes [12, 13]. CHF was characterized by activation of sympathetic nervous system, increased catecholamine concentration, declined expression of β_1-AR and β_2-AR and increased expression of β_3-AR. At earlier stages of CHF, the role of β_3-AR was to relieve the excessive positive inotropic effect of β_1-AR and β_2-AR to prevent myocardial damage. Therefore up-regulation of the β_3-AR could be a compensatory mechanism to prevent further cardiomyocyte injury. However, later on, an imbalance among the adrenoreceptors may promote further deterioration of heart function [14]. In recent years, some studies showed that in patients with CHF, vascular endothelial dysfunction is common and could in turn exacerbate the heart failure [15]. Given the role of endothelial cells dysfunction in CHF, whether β_3-AR expression associated with endothelial dysfunction remains unclear. In this study, we also investigated the effect of β_3-AR expression on endothelial function and the possible mechanisms underlying it.

Materials and methods

Materials

BRL 37344, SR 59230A, H-89, L-NAME, Propranolol, acetylcholine (Ach) were acquired from Sigma-Aldrich (St. Louis, MO, USA). Noradrenaline bitartrate was purchased from Jinyao AminoAcid Ltd, (Tianjin, China). β_3 primary antibody was purchased from Boyan Biotech Ltd (Shanghai, China), NF-κB p65 primary antibody was purchased from Cell Signaling Technology (Danvers, MA, USA). RNA Stabilization reagent, RNA zap, miRNeasy mini kit, miScript II RT Kit, miScript SYBR Green PCR kit and 96 panel miScript miRNA PCR arrays plates were all purchased from Qiagen (Germany). The SABC immunohistochemical kit was provided by BOSTER (Shanghai, China). CFX96 Real-time PCR was from BIO-RAD (Berkeley, CA, USA). RIPA extraction buffer, PMSF, BCA kit and SDS-PAGE gel were purchased from Beyotime (Guangzhou, China). ChemiDoc™ MP imaging system was provided by BIO-RAD, USA.

Animal models

Adult male Sprague-Dawley (SD) rats weighing 180-220 g were provided by the Experimental Animal Centre of Military Medical Sciences in Beijing. All animal care and experimental procedures followed ethical standards of animal use and were approved by Institutional Animal Care and Use Committee of Shanxi Medical University. The rats had free access to water and standard laboratory chow diet and were kept at a light/dark cycle of 12 hours at 20-22°C. The rats were divided into Sham group (n=70) and CHF group (n=130). Chronic heart failure (CHF) was produced by left coronary artery ligation. Briefly, SD rats were anaesthetized with chloral hydrate (10%, 0.3 ml·100 g^{-1}, Shanghai Biological Engineering Co Ltd) and ventilated by trachea cannula incubation. The heart was exposed by left thoracotomy and the descending coronary artery of the left anterior was ligated directly proximal to the main branching point. Then the thorax was closed, the rats were extubated immediately after their spontaneous respiration was sufficient and allowed to be recovered under strictly controlled conditions. The Sham group received an identical operation but without ligation. 20 rats from Sham group and 20 rats from CHF group were divided into four groups, Sham control group (n=10), Sham+SR group (n=10), CHF control group (n=10), CHF+SR group (n=10). Rats in SR application groups received intraperitoneal injection of 85 nmol SR 59230A in 1 ml saline twice a day for five weeks. Rats in control groups received intraperitoneal injection of 1 ml saline twice a day. The left rats in Sham group and CHF group were cared in the animal facilities for three more weeks.

Echocardiograph

Echocardiograms were recorded at the 4th week after the surgery. Rats were anaesthetized by intraperitoneal injection of chloral hydrate (10%, 0.3 ml·100 g^{-1}). Cardiac structure and function were assessed using transthoracic echocardiogram (vivid7/dimension, GE, USA). Detection parameters include: left ventricular diastolic diameter (LVIDd), left ventricular systolic diameter (LVIDs), left ventricular ejection fraction (LVEF) and left ventricular fractional shortening (LVFS). The results obtained were the mean values of three cardiac cycles.

H&E staining of the heart and aorta tissue

Rats from all groups were euthanized by overdose chloral hydrate. The heart was excised and washed with saline to remove the excess

Table 1. Echocardiographic values of chronic heart failure (CHF)

Grouping	LVIDd (mm)	LVIDs (mm)	EF (%)	FS (%)
Sham group (n=6)	5.12±0.47	3±0.33	78±4.2	41.17±3.92
CHF group (n=7)	6.58±1.05[b]	4.72±0.65[c]	59.71±8.26[c]	27.29±5.56[c]

Values are means ± SD. [b]*P*<0.05, [c]*P*<0.01 *vs.* Sham group.

connective tissues and blood. The bibulous paper was used to absorb the water on samples. The aorta rings were obtained with the same process and treatment. Then the heart and aorta rings were stored in formalin, embedded in paraffin and cut into slices at 6-μm thickness and dried in a thermostat at 37°C for 24 hours. The slices were transparented with dimethylbenzene and dehydrated with ethanol at gradient, then stained with hematoxylin-eosin (H&E), dehydrated and transparented again. Histopathologic images were obtained with the microscope (LEICA, Germany).

Thoracic aorta rings preparation and tension studies

After anaesthetized, the descending thoracic aorta of rats was isolated and dissected to prevent endothelium damage and placed immediately into the oxygenated ice-cold Krebs-Henseleit (Krebs) solution composed of (in mmol·L^{-1}): NaCl, 144; KCl, 5.8; glucose, 11.1; HEPES, 5.0; $MgCl_2$ 1.2; $CaCl_2$ 2.5 (pH 7.4). After removing fat and connective tissues, thoracic aorta was cut into 3-5 mm rings. In some rings, the endothelium was removed by gentle rubbing of the intimal surface with a fine cardellino. The aorta rings were then suspended on stainless-steel hooks in a 5 ml organ bath filled with a continuously oxygenated Krebs solution at 37°C (pH 7.4).

The aorta rings were progressively stretched to a tension of 2 g and allowed to equilibrate for 60 min with replacement of fresh Krebs solution every 15 min. After reaching equilibration, the vascular rings were tested for viability using 30 mmol·L^{-1} of KCl containing Krebs solution in which NaCl was partially replaced by an equimolar amount of KCl. Only vascular rings with less than 10% contraction differences were used for the experiments. The vascular tension was recorded through a force displacement transducer (ADI, USA).

The endothelial function of the aorta rings was tested by the presence of at least 70% relaxation in response to acetylcholine (Ach, 10^{-6} mol·L^{-1}) in rings pre-contracted with Noradrenaline (NA, 10^{-6} mol·L^{-1}). Endothelium free was confirmed by the absence of acetylcholine-induced relaxation. Functional and mechanism studies of β_3-AR in rat thoracic aorta were carried out by adding BRL 37344 (BRL), a specific β_3-AR agonist into the tissue bath after vasoconstriction reached a steady state in high concentration of KCl. The tension of the vascular rings was recorded in presence and/or absence of SR 59230A (SR), Propranolol, L-NAME and H-89 respectively.

Effect of SR 59230A on the endothelial function and vascular contractive response

Tissues from rats of the four groups were used to perform the following experiments. (1) Arterial diastolic responses to Ach: After the equilibration period, artery rings were constricted with NA (10^{-6} mol·L^{-1}). The integrity of the endothelium was tested with Ach (10^{-12}-10^{-4} mol·L^{-1}) when vasoconstriction reached a steady state. Then the cumulative concentration response curves to Ach were obtained. (2) Arterial contractive responses to NA: After 30 min of Ach wash out, the artery rings were constricted with NA (10^{-8}-10^{-5} mol·L^{-1}), wash out again when it reached a stable state followed by addition of 60 mmol·L^{-1} of KCl. Thoracic aortic vasoconstriction response was expressed by the percentage of contraction caused by NA and contraction induced by KCl. After that, a cumulative concentration-response curve to NA was constructed.

Immunohistochemistry (IHC)

Slices with paraffin embedded sections were deparaffined in dimethyl benzene twice, dehydrated with gradient ethanol followed by hydration. Then the slices were treated with 10% hydrogen peroxide for 10 min at room temperature to block endogenous peroxidase. After antigen retrieving and blocking, the slices were incubated with the primary antibody at 4°C overnight. The final concentration of anti-mouse β_3 receptor is 1:1000, anti-mouse NF-κB is 1:600. After that, the slices were incubated with secondary antibody at room temperature for 30 min, then with SABC for 20 min. The slices were colored using DAB (Zhong Shan-Golden

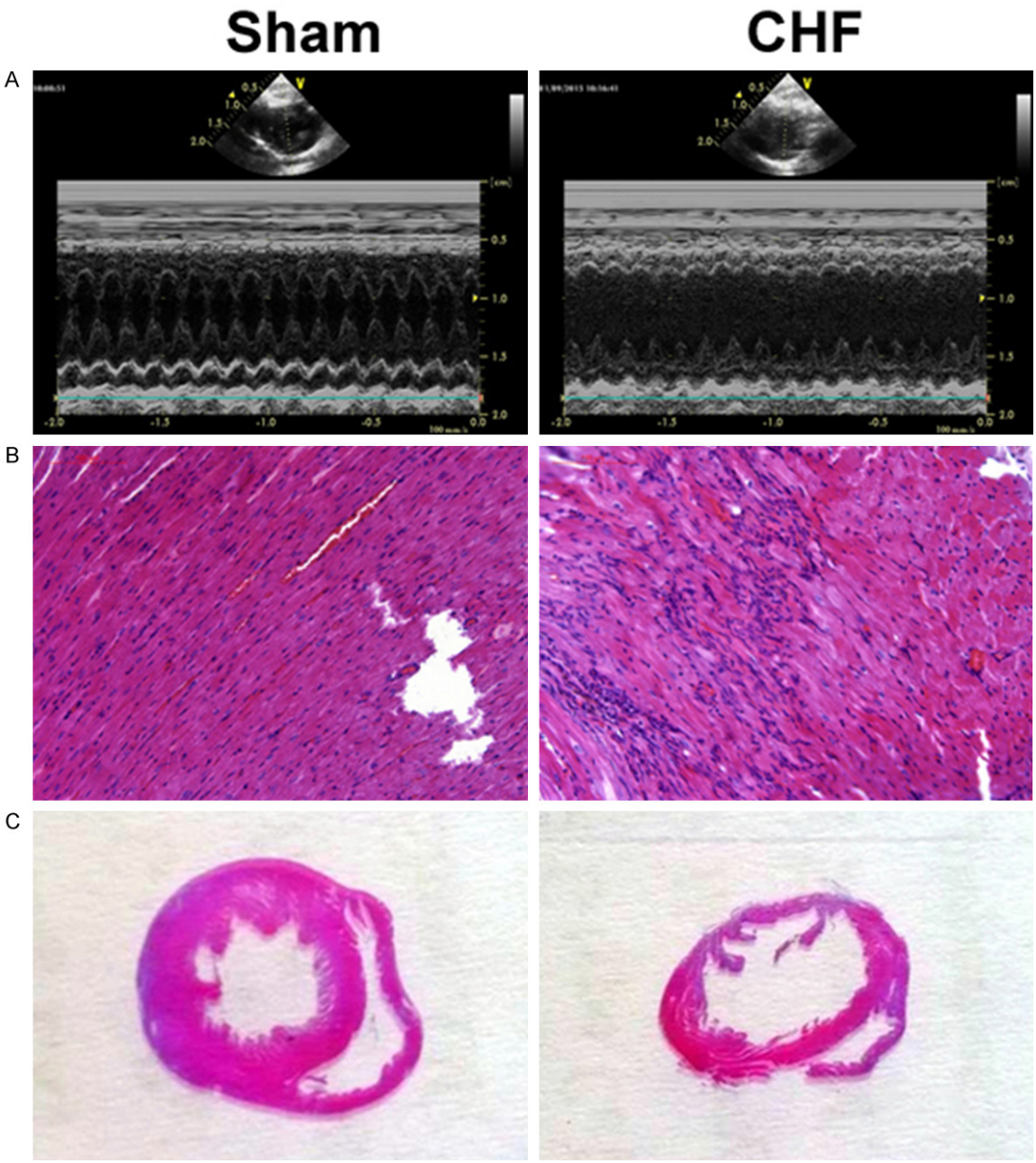

Figure 1. Establishment of chronic heart failure. A. Representative echocardiograms of Sham and CHF rats. B. Representative H&E staining of myocardial structure (×200). C. Ventricular cavity images of rats. Left panel: Sham rats; Right panel: CHF rats.

Bridge, China), hematoxylin stained, dehydrated, transparented and mounted with the resin. The positive granules appeared as brown particles. Standard for evaluation of IHC scoring is based on stain extent and intensity. The stain extent scoring was given from 0 to 4, where 0 was none observed and 4 was >80% of staining. The stain intensity grading was 0 to 3, where 0 represented non-staining and 3 represented the darkest brown staining.

Western blot

Standard western blotting procedures were carried out. The antibodies used were: NF-κB p65 primary antibody (1:1000; Cell Signaling

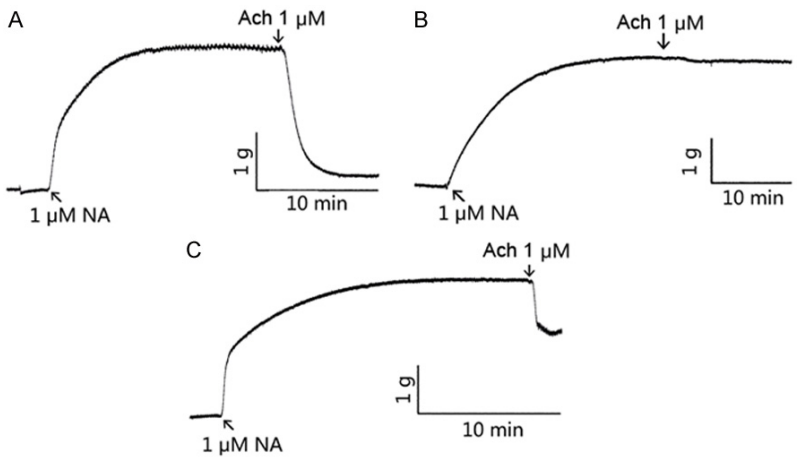

Figure 2. Detection of thoracic aorta endothelial integrity. A. Sham endothelium-intact group. B. Endothelium-free group. C. CHF endothelium-intact group.

Technology, US). ChemiDoc™ MP imaging system (BIO-RAD, USA) was used for exposure.

miScript miRNA PCR arrays

Thoracic aorta tissues from rats of the four groups were used for RNA isolation. Total RNA extraction was performed using miRNeasy Mini Kit according to the manufacturer's protocol. RNA concentration was determined by Nanodrop 2000c spectrophotometer (Thermo, USA). RNAs were stored at -80°C until use.

cDNA synthesis was carried out using the miScript II RT Kit. According to the manufacturer's protocol, the reverse transcription reaction system was incubated for 60 min at 37°C, followed by 5 min at 95°C. After the reverse transcription, cDNA were stored at -20°C for miScript miRNA PCR Arrays procedure within 1 week.

Real-time PCR was performed by using the miScript SYBR Green PCR kit. Template cDNAs were added into the reaction system and mixed well following the manufacturer's instructions. The 96 well plate was applied to screen the candidate microRNAs (miRNAs) which was centrifuged then placed in the CFX96 Real-time PCR machine in a reaction conditions of an initial activation of the DNA Polymerase for 15 min at 95°C, followed by 40 cycles of denaturation for 15 sec at 94°C, annealing for 30 sec at 55°C and extension for 30 sec at 70°C with the collection of the fluorescence data being performed during the extension step. The fold changes of miRNAs expression were calculated by the $2^{-\Delta\Delta CT}$ method.

Statistical analysis

Data are expressed as mean ± SD. Comparison of two treatment groups using two-tail unpaired student t-test with the SPSS program package (SPSS version 16.0). The values of $P<0.05$ were considered to be statistically significant.

Results

Establishment of heart failure model

The cardiac function was assessed by echocardiography (**Table 1** and **Figure 1**). Compared with the Sham group, EF% and FS% were significantly decreased in CHF group (59.71± 8.26% *vs.* 78±4.2%; 27.29±5.56% *vs.* 41.17± 3.92%, respectively, $P<0.01$) (**Table 1**). LVIDd and LVIDs were also significantly increased ($P<0.05$ and $P<0.01$ respectively) in CHF group, which indicated a decrease in the LV contractility (**Table 1**). In addition, cardiac systolic dysfunction was observed in CHF groups (**Figure 1A**). The myocardial structure in Sham group presented clear boundaries and regular arrangement, while the myocardial fibers were irregular and unclear in CHF group. Furthermore, the cardiomyocytes had neutrophils infiltration (**Figure 1B**) and expansion of left ventricular cavity, and left ventricular walls were thin in CHF group (**Figure 1C**).

Detection of endothelial integrity

The endothelial integrity was assessed by application of acetylcholine (Ach, 10^{-6} mol·L^{-1}) on aortic rings pre-contracted with Noradrenaline bitartrate incubation (NA, 10^{-6} mol·L^{-1}). For Sham rats, Ach induced a greater relaxation in endothelium-intact group, in endothelium-free group, the relaxant effect was inhibited. In addition, for endothelium-intact aorta rings, Ach induced more relaxation in Sham group than CHF group (**Figure 2**).

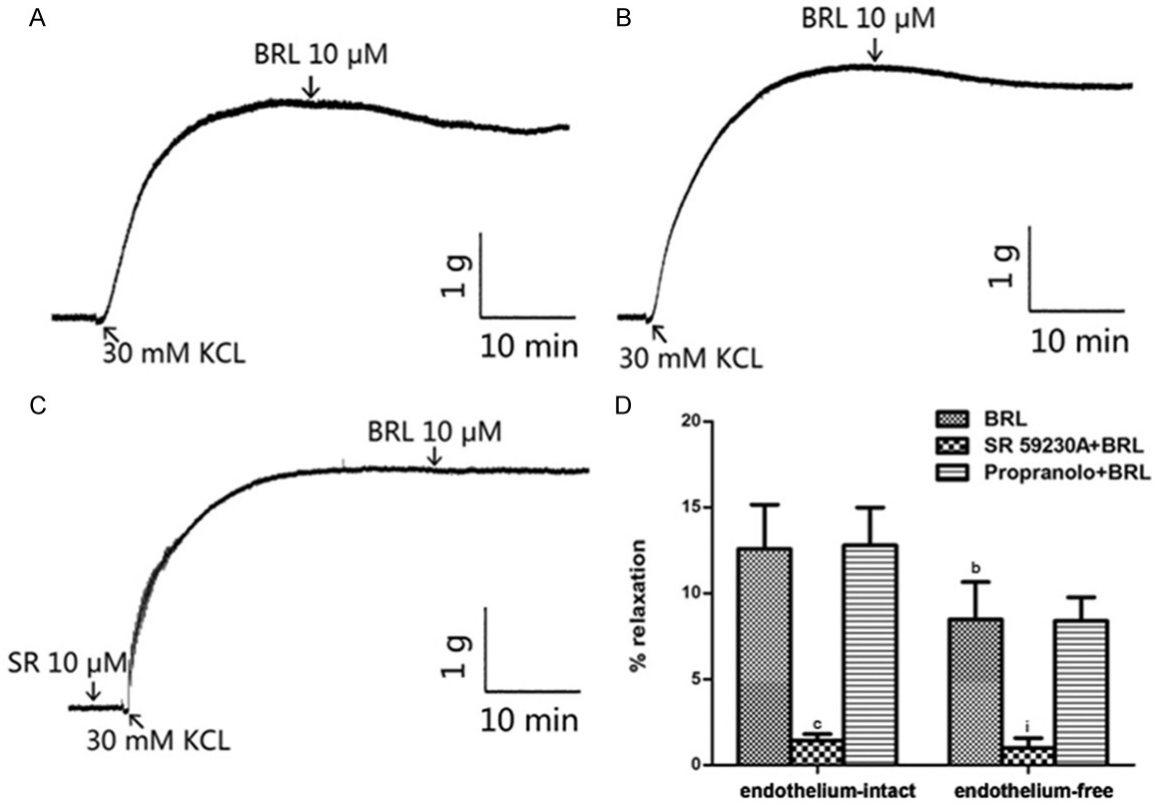

Figure 3. BRL relaxed both endothelium-intact and endothelium-free aorta. A. BRL relaxed thoracic aorta in endothelium-intact tissue. B. BRL relaxed aorta in endothelium-free tissue. C. Effect of SR on the relaxant effect of BRL in endothelium-free tissue. D. Mechanistic studies of BRL-induced vasodilation. Results are expressed as percentage of relaxation pre-contracted by 30 mmol·L-1 of KCl. Values were represented as mean ± SD. [b]*P*<0.05, [c]*P*<0.01 vs. Sham endothelium-intact BRL group. [i]*P*<0.01 *vs.* Sham endothelium-free BRL group.

Role of β_3-AR on thoracic aorta

BRL induced a vasorelaxation of 12.71±2.58% (n=6) (**Figure 3A**, **3D**) in endothelium-intact aorta rings and 8.78±1.83% (n=6) (**Figure 3B**, **3D**) in endothelium-free aorta rings (*P*<0.05). To elucidate if these actions are induced by activation of β_3-AR alone, the relaxation of BRL were also measured in the presence of Propranolo (the β_1- and β_2-ARs antagonist) and SR 59230A (SR, the β_3-AR antagonist). Propranolol pre-treatment had no effect on the relaxant effect of BRL in both endothelium-intact and endothelium-free aorta in Sham group (**Figure 3D**). After pre-treatment with SR, the relaxant ability of BRL was inhibited (**Figure 3C**, **3D**). The above results demonstrated that BRL relaxed the aorta ring through β_3-AR activation both in endothelium-intact and endothelium-free vessel.

Mechanisms of BRL 37344-induced relaxation in Sham rat aorta

The relaxant effect of BRL was remarkably attenuated by pre-treatment of L-NAME both in endothelium-intact (4.81±0.38%) (**Figure 4A**, **4B**) and endothelium-free groups (4.74±0.58%) (**Figure 4C**, **4D**). However, the effect of H-89 was not statistically significant (**Figure 4E**). In conclusion, vasodilation induced by β_3-AR was related to NO synthase pathway.

Vasodilation effect of β_3-AR on CHF rat aorta smooth muscle

Immunohistochemical staining showed that β_3-AR was distributed in thoracic aorta endothelium and a part of the smooth muscle in the Sham group (**Figure 5A**). The expression of β_3-AR was up-regulated significantly in the thoracic aorta smooth muscle in CHF group (**Figure 5A**).

BRL induced stronger relaxant effect in CHF aorta smooth muscle (13.4±1.9%, n=6, *P*< 0.01) (**Figure 5B**) than that in Sham aorta smooth muscle. L-NAME treatment reduced the relaxation effect to 2.23±0.77% (n=7, *P*<0.01) and H-89 application partially inhibited the vasodilation effect (n=6, *P*>0.05) (**Figure 5B**,

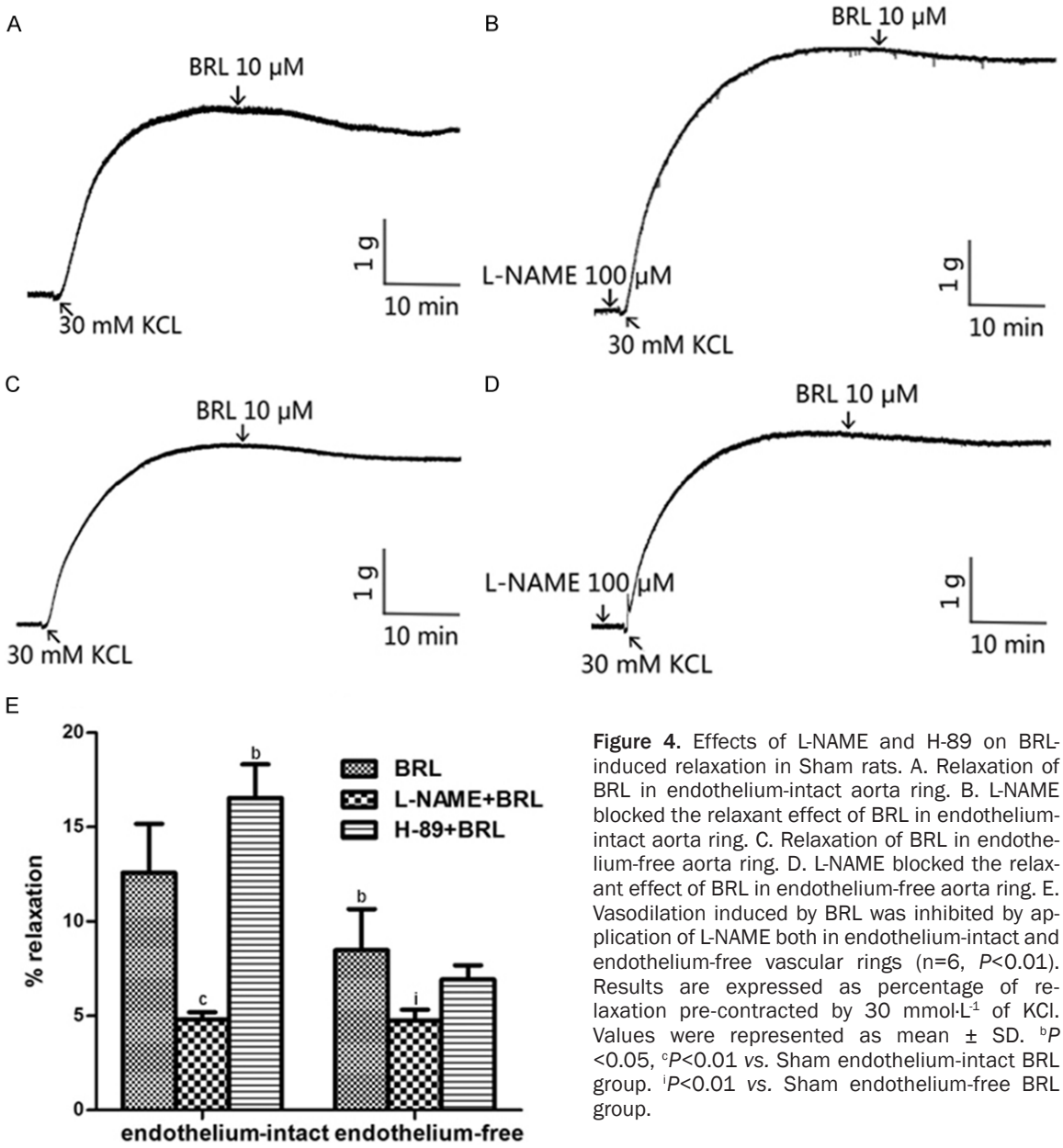

Figure 4. Effects of L-NAME and H-89 on BRL-induced relaxation in Sham rats. A. Relaxation of BRL in endothelium-intact aorta ring. B. L-NAME blocked the relaxant effect of BRL in endothelium-intact aorta ring. C. Relaxation of BRL in endothelium-free aorta ring. D. L-NAME blocked the relaxant effect of BRL in endothelium-free aorta ring. E. Vasodilation induced by BRL was inhibited by application of L-NAME both in endothelium-intact and endothelium-free vascular rings (n=6, $P<0.01$). Results are expressed as percentage of relaxation pre-contracted by 30 mmol·L^{-1} of KCl. Values were represented as mean ± SD. $^{b}P<0.05$, $^{c}P<0.01$ *vs.* Sham endothelium-intact BRL group. $^{i}P<0.01$ *vs.* Sham endothelium-free BRL group.

right). The Inhibitory effect of L-NAME was stronger in CHF aorta smooth muscle than that in Sham aorta smooth muscle. Taken together, during development of heart failure, the expression of β_3-AR in aorta smooth muscle was up-regulated to exert vasodilator effect which was related to the NOS pathway.

The effect of SR 59230A on rat thoracic aorta endothelial function and contractive response

Endothelial function and vascular contractive response were detected by vascular perfusion after five weeks intraperitoneal injection of SR *in vivo*. Sham+SR group showed a reduced endothelium-dependent relaxation response to Ach (Emax=73.79±8.3%, n=6 *vs.* Emax=90.22±6.15%, n=6, $P<0.01$) and an increased contraction response to NA (Emax=95.02±3.79%, n=8 *vs.* Emax=79.99±2.28% of Sham, n=6, $P<0.01$) (**Figure 6A**, **6C**); The concentration-dependent response to Ach in CHF control group was declined to 46.64±18.47% (n=6, $P<0.01$ *vs.* Sham control group) but was 63.67±10.8% (n=6, $P>0.05$ *vs.* CHF control group) after 5 weeks injection of SR (**Figure 6B**). Emax of the concentration-dependent response caused by NA in CHF control group

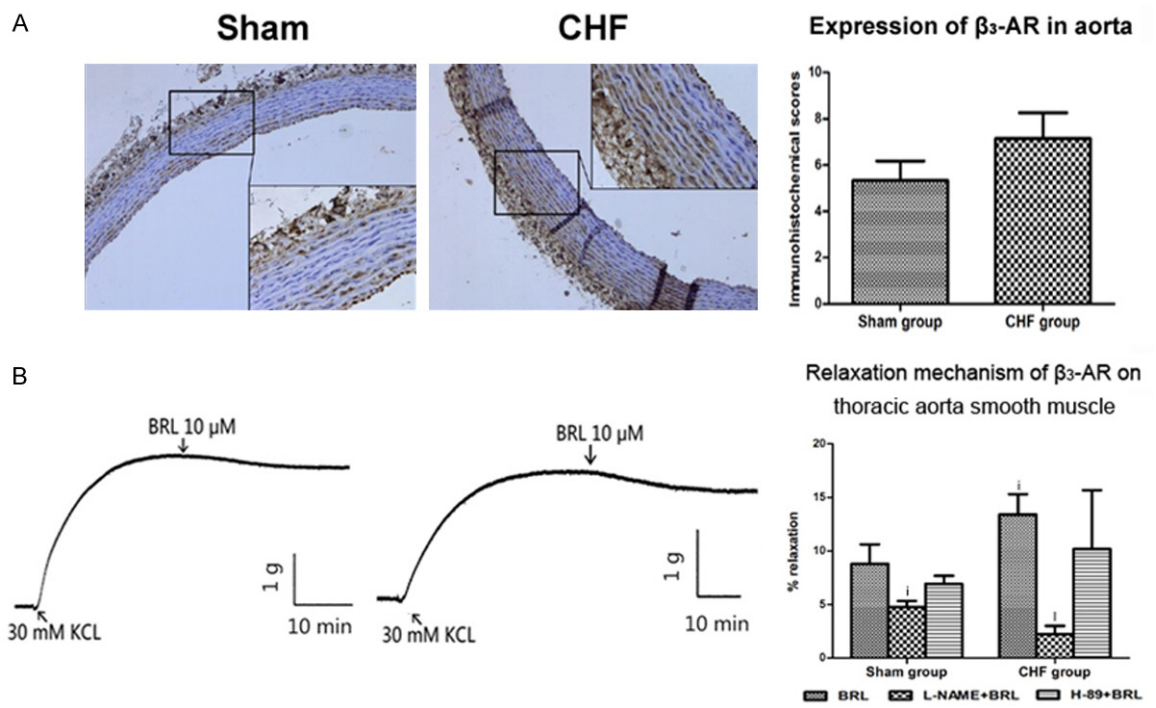

Figure 5. Expression of β_3-AR in rat thoracic aorta and its relaxation action. (β_3-AR immumohistochemical staining, original magnifcation, ×100; ×400). A. Left: Expression of β_3-AR in rat thoracic aorta of Sham group; Middle: Expression of β_3-AR in rat thoracic aorta of CHF group; Right: The immunohistochemical scores of the expression of β_3-AR. B. Mechanisms of vascular smooth relaxation mediated by β_3-AR activation. Left: Representative relaxation curve of aorta smooth muscle in Sham group; Middle: Representative relaxation curve of aorta smooth muscle in CHF group; Right: Mechanisms of β_3-AR activation induced relaxation of smooth muscle in CHF group. Results are expressed as percentage of relaxation pre-contracted by 30 mmol·L^{-1} of KCl. Values were represented as mean ± SD. $^{i}P<0.01$ vs. Sham endothelium-free BRL group. $^{I}P<0.01$ vs. CHF endothelium-free BRL group.

was increased to 90.75±8.29% (n=6, *P*<0.05) and increased to 100.32±4.76% (n=6, P<0.05 *vs.* CHF control group) after 5 weeks injection of SR (**Figure 6D**). These results indicated that β_3-AR mediates the relaxant effect in rat thoracic aorta and inhibition of β_3-AR induced endothelial injury in Sham rat's aorta, but delayed the damage of aorta caused by CHF to some extent after injection of SR.

Structural changes of rat thoracic aorta and NF-κB expression

In Sham control group, the endothelial cells were intact, smooth muscle cells in the tunica media were arranged in order with clear structure of blood vessel wall. In Sham+SR group, the tunica intima lost integrality with thickened tunica media and disordered arrangement of elastic fibers. In CHF control group, smooth muscle cells in the tunica media were disorganized and proliferated with obvious endothelial denudation, while in the CHF+SR group, arrangement of the smooth muscle cells was relatively regular (**Figure 7A**).

NF-κB expression in aorta was performed using immunohistochemistry analysis and western blot (**Figure 7B-E**). The expression of NF-κB in aorta was increased a little in Sham+SR group compared to the Sham control group, NF-κB immunostaining was stronger in the CHF group (**Figure 7B**, **7C**), indicated an increased expression of NF-κB in development of heart failure. After 5 weeks of in vivo SR application, the expression of NF-κB in CHF rat aorta reduced, coinciding with the functional studies mentioned above (**Figure 6**).

Role of β_3-AR on the expression profiles of miRNAs in rat thoracic aorta

After extracting RNAs from rat thoracic aorta of the SR-untreated and -treated rats with or without heart failure, we did a microarray screening to evaluate the expression patterns of miR-

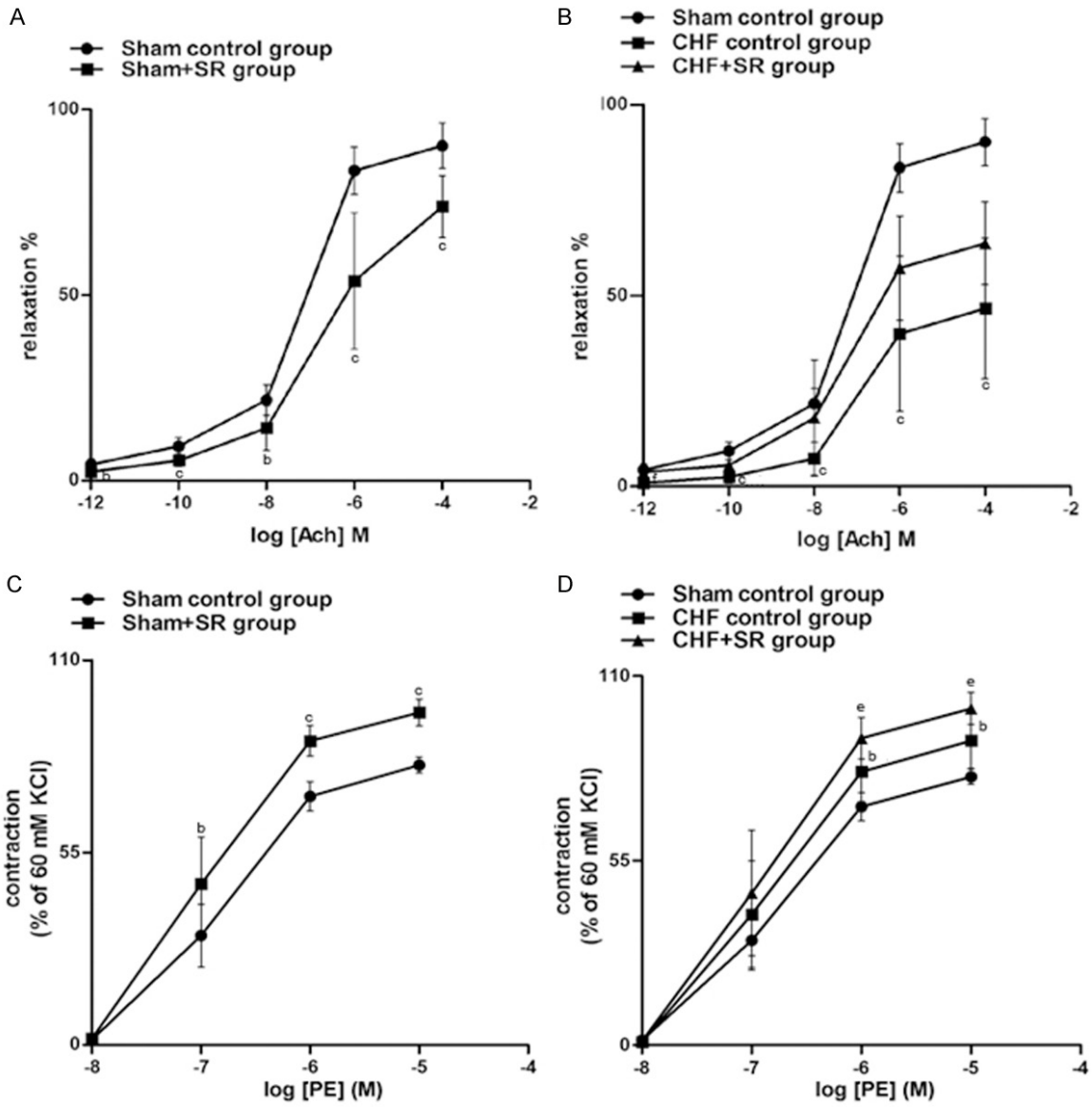

Figure 6. Influence of *in vivo* SR application on endothelial function and contractive response of rat thoracic aorta. A. Effect of SR on vascular endothelial function in Sham group. B. Effect of SR on vascular endothelial function in CHF group. C. Effect of SR on vascular contractive response in Sham group. D. Effect of SR on vascular contractive response in CHF group. Values were mean ± SD. $^{b}P<0.05$, $^{c}P<0.01$ *vs*. Sham control group. $^{e}P<0.05$, $^{f}P<0.01$ *vs*. CHF control group.

NAs. The results showed 14 up-regulated miRNAs and 34 down-regulated miRNAs in Sham +SR group (**Figure 8A**, **8B**). Under heart failure condition, there were 23 miRNAs up-regulated and 19 miRNAs down-regulated (**Figure 8C**, **8D**). Among them, the expression of 25 miRNAs changed after 5 weeks injection of SR. We identified 9 up-regulated miRNAs and 16 down-regulated miRNAs that are related to β_3-AR inhibition both in Sham and CHF rat aortas (**Figure 8E**, **8F**; **Table 2**). After literature research, 19 of them were found to be related to NF-κB pathway (**Table 2**), among them expression of rno-miR-451-5p and rno-let-7c-5p reached a statistical significance.

Discussion

Several reports pointed out that β_3-AR agonist SR 58611 and a selective β-adrenoceptor (β_1-AR) antagonist nebivolol exhibited relaxation effect in rat thoracic aorta, and the effect was blocked in the presence of β_3-AR antagonists such as L-748, 377 or SR 59230A [9, 32]. All of

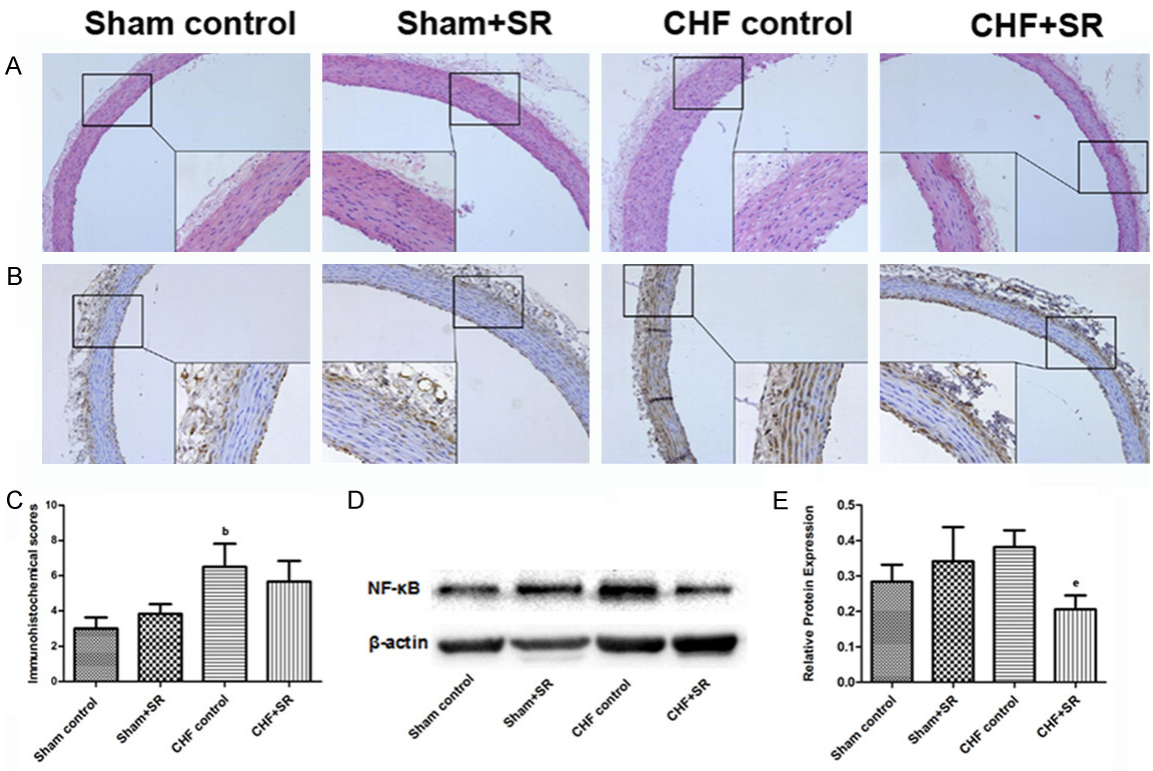

Figure 7. Structure and NF-κB expression of rat thoracic aorta. A. H&E staining of rat thoracic aorta. (Outside, ×100; inside, ×400). B. NF-κB expression in rat thoracic aorta. C. The immunohistochemical scores of NF-κB expression in rat thoracic aorta. D. Western blot result of NF-κB expression. E. Relative gray value of NF-κB blots to β-actin. [b]*P*<0.05 *vs.* Sham control group, [e]*P*<0.05 *vs.* CHF control group.

these results suggested that β_3 receptor exists in the aorta with vasodilation effect, consistent with our observation in the present study showing that BRL 37344, a specific β_3-AR agonist, could induce a relaxant effect in rat thoracic aorta through activation of a NO synthase pathway.

The relaxant effect of BRL 37344 had been investigated in isolated common carotid arteries of the rat [33] and smooth muscle of the gastrointestinal tract before [34, 35]. However, the localization of β_3-AR in rat thoracic aortic has not been defined with controversial results among different studies. Trochu et al. indicated that isoprenaline-induced relaxation in aortic rings after endothelium removal, but only at higher concentrations and pretreatment of nadolol abolished this relaxant effect [9]. However, RT-PCR analysis detected β_3-AR transcripts both in thoracic aorta and freshly isolated endothelial cells [36]. To resolve the discrepancy, immunohistochemical staining with a specific anti-β_3-AR monoclonal antibody was used in this study and showed that β_3-AR was distributed in both rat thoracic aorta endothelium and smooth muscle layer.

Previous studies demonstrated that β_3-AR-mediated the negative inotropic effect was via a nitric oxide synthase (NOS)/nitric oxide (NO)/soluble guanylate cyclase (sGC)/cGMP pathway in cardiomyocytes [6]. Others reported that activation of β_3-AR was through $G\alpha_s$/cAMP/PKA pathway in the portal vein myocytes of rat [37] and pre-treatment with L-NMMA partially inhibited isoprenaline-induced relaxation, in addition, SR 58611 also produced a slight relaxation in the presence of L-NMMA [9]. To investigate the role of NO synthase and PKA pathway in vasorelaxation induced by β_3-AR activation, aorta rings were pre-incubated with L-NAME and H-89 (PKA blocker) separately in this research and showed that the relaxant action of BRL was remarkably attenuated by pre-treatment with L-NAME on endothelium-intact and endothelium-free aorta rings. However, H-89 slightly inhibited the vasodilation of the endothelium-free samples. All the

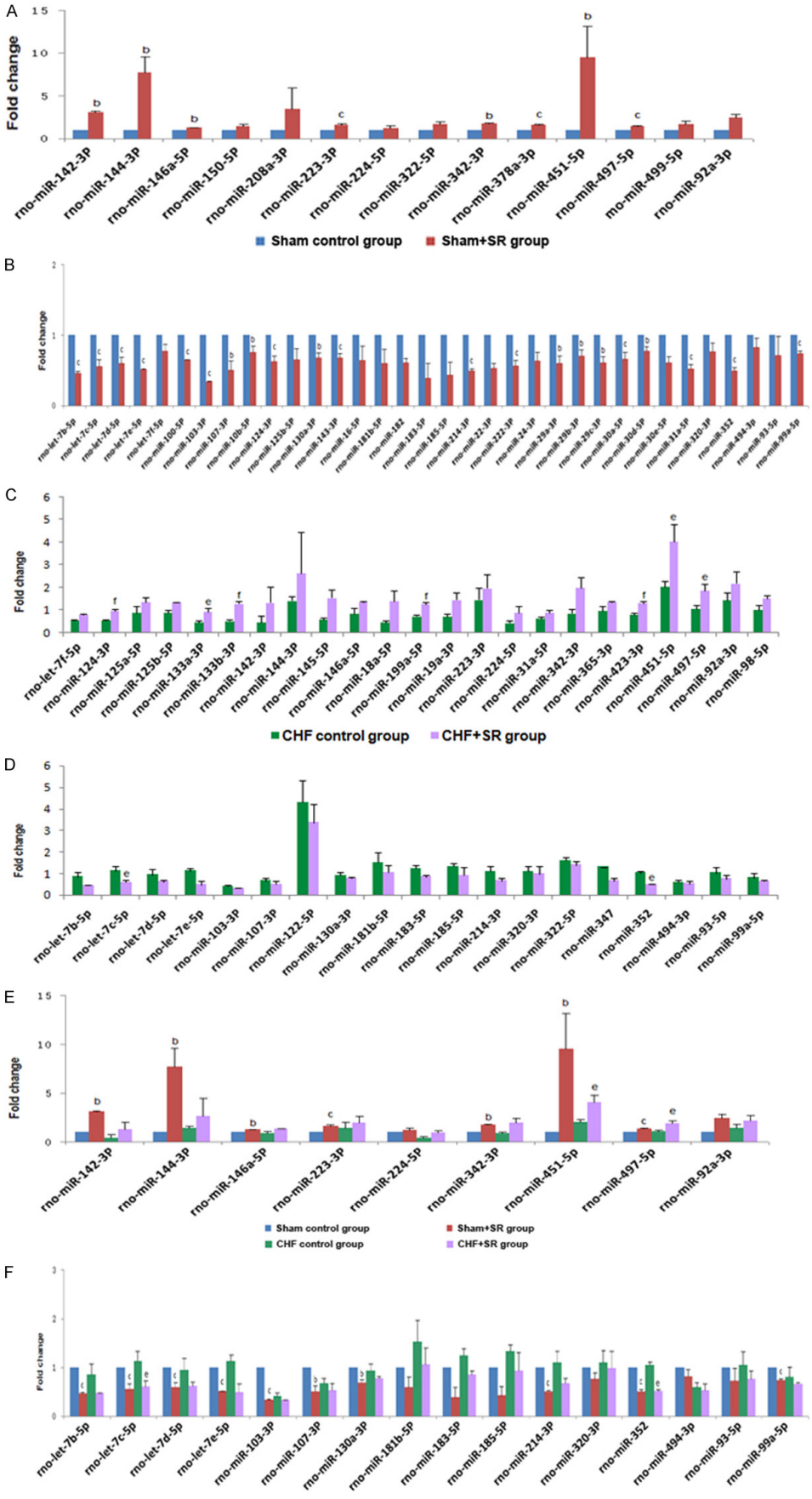
A
Fold change
rno-miR-142-3P
rno-miR-144-3P
rno-miR-146a-5P
rno-miR-150-5P
rno-miR-208a-3P
rno-miR-223-3P
rno-miR-224-5P
rno-miR-322-5P
rno-miR-342-3P
rno-miR-378a-3P
rno-miR-451-5P
rno-miR-497-5P
rno-miR-499-5P
rno-miR-92a-3P
Sham control group
Sham+SR group
B
Fold change
C
Fold change
rno-let-7f-5p
rno-miR-124-3P
rno-miR-125a-5P
rno-miR-125b-5P
rno-miR-133a-3P
rno-miR-133b-3P
rno-miR-142-3P
rno-miR-144-3P
rno-miR-145-5P
rno-miR-146a-5P
rno-miR-18a-5P
rno-miR-199a-5P
rno-miR-19a-3P
rno-miR-223-3P
rno-miR-224-5P
rno-miR-31a-5P
rno-miR-342-3P
rno-miR-365-3P
rno-miR-423-3P
rno-miR-451-5P
rno-miR-497-5P
rno-miR-92a-3P
rno-miR-98-5P
CHF control group
CHF+SR group
D
Fold change
rno-let-7b-5p
rno-let-7c-5p
rno-let-7d-5p
rno-let-7e-5p
rno-miR-103-3P
rno-miR-107-3P
rno-miR-122-5P
rno-miR-130a-3P
rno-miR-181b-5P
rno-miR-183-5P
rno-miR-185-5P
rno-miR-214-3P
rno-miR-320-3P
rno-miR-322-5P
rno-miR-347
rno-miR-352
rno-miR-494-3P
rno-miR-93-5P
rno-miR-99a-5P
E
Fold change
rno-miR-142-3P
rno-miR-144-3P
rno-miR-146a-5P
rno-miR-223-3P
rno-miR-224-5P
rno-miR-342-3P
rno-miR-451-5P
rno-miR-497-5P
rno-miR-92a-3P
Sham control group
Sham+SR group
CHF control group
CHF+SR group
F
Fold change
rno-let-7b-5p
rno-let-7c-5p
rno-let-7d-5p
rno-let-7e-5p
rno-miR-103-3P
rno-miR-107-3P
rno-miR-130a-3P
rno-miR-181b-5P
rno-miR-183-5P
rno-miR-185-5P
rno-miR-214-3P
rno-miR-320-3P
rno-miR-352
rno-miR-494-3P
rno-miR-93-5P
rno-miR-99a-5P

Figure 8. Expression of miRNAs in rat aorta. A, B. Expression of miRNAs in Sham and Sham+SR group. C, D. Expression of miRNAs in CHF and CHF+SR group. E, F. Expression of altered miRNAs after SR administration in rat aorta. [b]*P*<0.05, [c]*P*<0.01 *vs.* Sham control group. [e]*P*<0.05, [f]*P*<0.01 *vs.* CHF control group.

Table 2. miRNAs related to β_3-AR inhibition

miRNA	Up-regulated	Down-regulated	Related to NF-κB
rno-miR-142-3p[b]	[b]*p*<0.05		Yes [16]
rno-miR-144-3p[b]	[b]*p*<0.05		Yes [17]
rno-miR-146a-5p[b]	[b]*p*<0.05		Yes [18]
rno-miR-223-3p[c]	[c]*p*<0.01		Yes [19]
rno-miR-224-5p			Yes [20]
rno-miR-342-3p[b]	[b]*p*<0.05		Yes [21]
rno-miR-451-5p[b,e]	[b]*p*<0.05, [e]*p*<0.05		Yes [22]
rno-miR-497-5p[c,e]	[c]*p*<0.01, [e]*p*<0.05		
rno-miR-92a-3p			Yes [23]
rno-let-7b-5p[c]		[c]*P*<0.01	Yes [24]
rno-let-7c-5p[c,e]		[c]*P*<0.01, [e]*P*<0.05	Yes [24]
rno-let-7d-5p[c]		[c]*P*<0.01	Yes [24]
rno-let-7e-5p[c]		[c]*P*<0.01	Yes [24]
rno-miR-103-3p[c]		[c]*P*<0.01	Yes [25]
rno-miR-107-3p[b]		[b]*P*<0.05	
rno-miR-130a-3p[b]		[b]*P*<0.05	Yes [26]
rno-miR-181b-5p			Yes [27]
rno-miR-183-5p			Yes [28]
rno-miR-185-5p			
rno-miR-214-3p[c]		[c]*P*<0.01	Yes [29]
rno-miR-320-3p			
rno-miR-352[c,e]		[c]*P*<0.01, [e]*P*<0.05	
rno-miR-494-3p			Yes [30]
rno-miR-93-5p			Yes [31]
rno-miR-99a-5p[c]		[c]*P*<0.01	

[b]*P*<0.05, [c]*P*<0.01 *vs.* Sham control group. [e]*P*<0.05 *vs.* CHF control group.

results suggested that β_3-AR-mediated vascular relaxation was related to the NO synthase-dependent pathway.

Accumulating evidences suggested that β_3-AR is activated at higher concentrations of catecholamines, and plays a negative inotropic role in heart [14]. Cardiovascular diseases, especially the chronic heart failure were associated with increased tissue and circulating catecholamines which mediate β_3-AR up-regulation in vivo [38]. When heart failure happened, the vessels will be in high catecholamine environment, possibly leading to up-regulation of β_3-AR in the vessels. In this study, we showed the different expressions of β_3-AR in thoracic aorta between control (Sham group) and heart failure rats (CHF group). Meanwhile, BRL induced a stronger vasodilation effect on thoracic aorta smooth muscle in heart failure rats than Sham rats and the expression of β_3-AR was significantly up-regulated in thoracic aorta smooth muscle of heart failure rats. Researchers speculated that up-regulation of β_3-AR in failing heart may counterbalance the harmful effects of the β_1-AR and perhaps be beneficial in the early stages of heart failure, although ultimately leading to myocardium damage [14, 39]. Chronic heart failure led to endothelial diastolic dysfunction. In the present study, we also evaluated the role of β_3-AR in vascular function and showed that SR 59230A injection enhanced the contractive response of rat thoracic aorta, and inhibition of β_3-AR led to endothelial injury in Sham rats. However, under CHF condition, SR 59230A administration no longer induces endothelium damage possibly due to inhibition of β_3-AR.

The transcription factor NF-κB was reported playing an important role in regulating inflammatory reactions, proliferation after vascular injury [40, 41]. In the study, through measuring the expression of NF-κB, we found that its expression was increased after SR treatment and highest NF-κB expression in CHF rats, suggesting vascular injury accompanied by the release of NF-κB. However, SR administration reversed the high expression of NF-κB in CHF rat aorta indicating the association of NF-κB with β_3-AR. Consistent with this, 19 differentially expressed miRNAs were identified in rat thoracic aorta with and without chronic heart failure related to β_3-AR to be associated with NF-κB signaling pathway. However, the exact mechanism by how β_3-AR is associated with NF-κB signaling remains unclear and requires further investigation.

In conclusion, our results confirmed that β_3-AR are expressed in rat aorta and exerts a relaxant effect through NOS-dependent pathway. Inhibition of β_3-AR delayed the damage of vessels in the development of heart failure possibly through regulation of NF-κB signaling pathway.

Acknowledgements

This study was supported by grants from the Natural Science Foundation of Shanxi Province (No. 2012011040-8), the National Natural Science Foundation of China (No. 81272695), the Science and Technology Innovation Fund of Shanxi Medical University (No. [2012] 11) and the Natural Science Foundation of Shanxi Province (No. 201601D11107).

Disclosure of conflict of interest

None.

Address correspondence to: Xiangli Cui, Department of Physiology, Shanxi Medical University, 56 Xinjiannan Road, Mailbox 903, Taiyuan 030001, Shanxi, China. Tel: +86-351-4135329; E-mail: sunscisci@sina.com

References

[1] Emorine LJ, Marullo S, Briend-Sutren MM, Patey G, Tate K, Delavier-Klutchko C, Strosberg AD. Molecular characterization of the human beta 3-adrenergic receptor. Science 1989; 245: 1118-1121.

[2] Carpene C, Chalaux E, Lizarbe M, Estrada A, Mora C, Palacin M, Zorzano A, Lafontan M, Testar X. Beta 3-adrenergic receptors are responsible for the adrenergic inhibition of insulin-stimulated glucose transport in rat adipocytes. Biochem J 1993; 296: 99-105.

[3] Manara L, Croci T, Landi M. Beta 3-adrenoceptors and intestinal motility. Fundam Clin Pharmacol 1995; 9: 332-342.

[4] Martin CA, Advenier C. Beta 3-adrenoceptors and airways. Fundam Clin Pharmacol 1995; 9: 114-118.

[5] Gauthier C, Tavernier G, Charpentier F, Langin D, Le Marec H. Functional beta3-adrenoceptor in the human heart. J Clin Invest 1996; 98: 556-562.

[6] Gauthier C, Leblais V, Kobzik L, Trochu JN, Khandoudi N, Bril A, Balligand JL, Le Marec H. The negative inotropic effect of beta3-adrenoceptor stimulation is mediated by activation of a nitric oxide synthase pathway in human ventricle. J Clin Invest 1998; 102: 1377-1384.

[7] Hristov KL, Cui X, Brown SM, Liu L, Kellett WF, Petkov GV. Stimulation of beta3-adrenoceptors relaxes rat urinary bladder smooth muscle via activation of the large-conductance Ca2+-activated K+ channels. Am J Physiol Cell Physiol 2008; 295: C1344-1353.

[8] Bardou M, Loustalot C, Cortijo J, Simon B, Naline E, Dumas M, Esteve S, Croci T, Chalon P, Frydman R, Sagot P, Manara L, Morcillo EJ, Advenier C. Functional, biochemical and molecular biological evidence for a possible beta(3)-adrenoceptor in human near-term myometrium. Br J Pharmacol 2000; 130: 1960-1966.

[9] Trochu JN, Leblais V, Rautureau Y, Beverelli F, Le Marec H, Berdeaux A, Gauthier C. Beta 3-adrenoceptor stimulation induces vasorelaxation mediated essentially by endothelium-derived nitric oxide in rat thoracic aorta. Br J Pharmacol 1999; 128: 69-76.

[10] Brahmadevara N, Shaw AM, MacDonald A. Evidence against beta 3-adrenoceptors or low affinity state of beta 1-adrenoceptors mediating relaxation in rat isolated aorta. Br J Pharmacol 2003; 138: 99-106.

[11] Brahmadevara N, Shaw AM, MacDonald A. ALpha1-adrenoceptor antagonist properties of CGP 12177A and other beta-adrenoceptor ligands: evidence against beta(3)- or atypical beta-adrenoceptors in rat aorta. Br J Pharmacol 2004; 142: 781-787.

[12] Lohse MJ, Engelhardt S, Eschenhagen T. What is the role of beta-adrenergic signaling in heart failure? Circ Res 2003; 93: 896-906.

[13] Lefkowitz RJ, Rockman HA, Koch WJ. Catecholamines, cardiac beta-adrenergic receptors, and heart failure. Circulation 2000; 101: 1634-1637.

[14] Gauthier C, Seze-Goismier C, Rozec B. Beta 3-adrenoceptors in the cardiovascular system. Clin Hemorheol Microcirc 2007; 37: 193-204.

[15] Ciccone MM, Iacoviello M, Puzzovivo A, Scicchitano P, Monitillo F, De Crescenzo F, Caragnano V, Sassara M, Quistelli G, Guida P, Favale S. Clinical correlates of endothelial function in chronic heart failure. Clin Res Cardiol 2011; 100: 515-521.

[16] Xu G, Zhang Z, Wei J, Zhang Y, Guo L, Liu X. microR-142-3p down-regulates IRAK-1 in response to Mycobacterium bovis BCG infection in macrophages. Tuberculosis (Edinb) 2013; 93: 606-611.

[17] Csiszar A, Gautam T, Sosnowska D, Tarantini S, Banki E, Tucsek Z, Toth P, Losonczy G, Koller A, Reglodi D, Giles CB, Wren JD, Sonntag WE, Ungvari Z. Caloric restriction confers persistent anti-oxidative, pro-angiogenic, and anti-inflammatory effects and promotes anti-aging miRNA expression profile in cerebromicrovascular endothelial cells of aged rats. Am J Physiol Heart Circ Physiol 2014; 307: H292-306.

[18] Li K, Ching D, Luk FS, Raffai RL. Apolipoprotein E enhances microRNA-146a in monocytes and macrophages to suppress nuclear factor-kappaB-driven inflammation and atherosclerosis. Circ Res 2015; 117: e1-e11.
[19] Liu Y, Wang R, Jiang J, Yang B, Cao Z, Cheng X. miR-223 is upregulated in monocytes from patients with tuberculosis and regulates function of monocyte-derived macrophages. Mol Immunol 2015; 67: 475-481.
[20] Liang M, Yao G, Yin M, Lu M, Tian H, Liu L, Lian J, Huang X, Sun F. Transcriptional cooperation between p53 and NF-kappaB p65 regulates microRNA-224 transcription in mouse ovarian granulosa cells. Mol Cell Endocrinol 2013; 370: 119-129.
[21] Zhao L, Zhang Y. miR-342-3p affects hepatocellular carcinoma cell proliferation via regulating NF-kappaB pathway. Biochem Biophys Res Commun 2015; 457: 370-377.
[22] Chen LJ, Chuang L, Huang YH, Zhou J, Lim SH, Lee CI, Lin WW, Lin TE, Wang WL, Chen L, Chien S, Chiu JJ. MicroRNA mediation of endothelial inflammatory response to smooth muscle cells and its inhibition by atheroprotective shear stress. Circ Res 2015; 116: 1157-1169.
[23] Zhang B, Zhou M, Li C, Zhou J, Li H, Zhu D, Wang Z, Chen A, Zhao Q. MicroRNA-92a inhibition attenuates hypoxia/reoxygenation-induced myocardiocyte apoptosis by targeting Smad7. PLoS One 2014; 9: e100298.
[24] Iliopoulos D, Hirsch HA, Struhl K. An epigenetic switch involving NF-kappaB, Lin28, Let-7 MicroRNA, and IL6 links inflammation to cell transformation. Cell 2009; 139: 693-706.
[25] Huang HC, Yu HR, Huang LT, Chen RF, Lin IC, Ou CY, Hsu TY, Yang KD. miRNA-125b regulates TNF-alpha production in CD14+ neonatal monocytes via post-transcriptional regulation. J Leukoc Biol 2012; 92: 171-182.
[26] Zhang J, Wu H, Li P, Zhao Y, Liu M, Tang H. NF-kappaB-modulated miR-130a targets TNF-alpha in cervical cancer cells. J Transl Med 2014; 12: 155.
[27] Wang Y, Mao G, Lv Y, Huang Q, Wang G. MicroRNA-181b stimulates inflammation via the nuclear factor-kappaB signaling pathway in vivo. Exp Ther Med 2015; 10: 1584-1590.
[28] Sha F, Wu S, Zhang H, Guo X. MiR-183 potentially inhibits NF-kappaB1 expression by directly targeting its 3'-untranslated region. Acta Biochim Biophys Sin (Shanghai) 2014; 46: 991-996.
[29] Duan Q, Wang X, Gong W, Ni L, Chen C, He X, Chen F, Yang L, Wang P, Wang DW. ER stress negatively modulates the expression of the miR-199a/214 cluster to regulates tumor survival and progression in human hepatocellular cancer. PLoS One 2012; 7: e31518.
[30] Ramachandran S, Karp PH, Osterhaus SR, Jiang P, Wohlford-Lenane C, Lennox KA, Jacobi AM, Praekh K, Rose SD, Behlke MA, Xing Y, Welsh MJ, McCray PB Jr. Post-transcriptional regulation of cystic fibrosis transmembrane conductance regulator expression and function by microRNAs. Am J Respir Cell Mol Biol 2013; 49: 544-551.
[31] Jiang Y, Zhu Y, Wang X, Gong J, Hu C, Guo B, Zhu B, Li Y. Temporal regulation of HIF-1 and NF-kappaB in hypoxic hepatocarcinoma cells. Oncotarget 2015; 6: 9409-9419.
[32] Rozec B, Quang TT, Noireaud J, Gauthier C. Mixed beta3-adrenoceptor agonist and alpha1-adrenoceptor antagonist properties of nebivolol in rat thoracic aorta. Br J Pharmacol 2006; 147: 699-706.
[33] Oriowo MA. Atypical beta-adrenoceptors in the rat isolated common carotid artery. Br J Pharmacol 1994; 113: 699-702.
[34] McLaughlin DP, MacDonald A. Evidence for the existence of 'atypical' beta-adrenoceptors (beta 3-adrenoceptors) mediating relaxation in the rat distal colon in vitro. Br J Pharmacol 1990; 101: 569-574.
[35] McLaughlin DP, MacDonald A. Characterization of catecholamine-mediated relaxations in rat isolated gastric fundus: evidence for an atypical beta-adrenoceptor. Br J Pharmacol 1991; 103: 1351-1356.
[36] Rautureau Y, Toumaniantz G, Serpillon S, Jourdon P, Trochu JN, Gauthier C. Beta 3-adrenoceptor in rat aorta: molecular and biochemical characterization and signalling pathway. Br J Pharmacol 2002; 137: 153-161.
[37] Viard P, Macrez N, Coussin F, Morel JL, Mironneau J. Beta-3 adrenergic stimulation of L-type Ca(2+) channels in rat portal vein myocytes. Br J Pharmacol 2000; 129: 1497-1505.
[38] Germack R, Dickenson JM. Induction of beta3-adrenergic receptor functional expression following chronic stimulation with noradrenaline in neonatal rat cardiomyocytes. J Pharmacol Exp Ther 2006; 316: 392-402.
[39] Pott C, Brixius K, Bloch W, Ziskoven C, Napp A, Schwinger RH. Beta3-adrenergic stimulation in the human heart: signal transduction, functional implications and therapeutic perspectives. Pharmazie 2006; 61: 255-260.
[40] Jeong IK, Oh DH, Park SJ, Kang JH, Kim S, Lee MS, Kim MJ, Hwang YC, Ahn KJ, Chung HY, Chae MK, Yoo HJ. Inhibition of NF-kappaB prevents high glucose-induced proliferation and plasminogen activator inhibitor-1 expression in vascular smooth muscle cells. Exp Mol Med 2011; 43: 684-692.
[41] Wrighton CJ, Hofer-Warbinek R, Moll T, Eytner R, Bach FH, de Martin R. Inhibition of endothelial cell activation by adenovirus-mediated expression of I kappa B alpha, an inhibitor of the transcription factor NF-kappa B. J Exp Med 1996; 183: 1013-1022.